ELSEVIER

Chemical Engineering Science 59 (2004) 2947–2960

Chemical Engineering Science

www.elsevier.com/locate/ces

The effects of diffusion mechanism and void structure on transport rates and tortuosity factors in complex porous structures

Jeffrey M. Zalc[a], Sebastián C. Reyes[b], Enrique Iglesia[a,*]

[a] *Department of Chemical Engineering, University of California at Berkeley, Berkeley, CA 94720-1462, USA*
[b] *ExxonMobil Research and Engineering Co., Route 22 East, Annandale, NJ 08801, USA*

Received 27 October 2003; received in revised form 19 April 2004; accepted 22 April 2004

Abstract

Tracer diffusion simulations within random porous structures show that tortuosity factors are independent of diffusion mechanism for all practical void fractions when an equivalent Knudsen diffusivity is correctly defined. Previous studies concluded that tortuosity factors, a geometric property of the void space as defined, increase with increasing Knudsen number, K_n, a measure of the relative number of molecule-surface and intermolecular collisions. The model porous structures in this study consist of random–loose packings of spheres overlapped to achieve a given void fraction and to accurately reflect the void space in practical porous solids. Effective diffusivities were estimated using tracer or flux-based Monte Carlo methods for Knudsen numbers of 10^{-3}–10^{10}; the two methods lead to similar diffusivities for void fractions of 0.06–0.42. Tortuosity factors estimated using the number-averaged distance between collisions, $\langle l_p \rangle$, for the characteristic void length scale increased with increasing Knudsen number, even though simulations in infinite cylinders confirmed the accuracy of the Bosanquet equation for all values of K_n. These unexpected changes in a geometric property of the void space become most apparent near the percolation void fraction ($\sim$0.04). For example, the Knudsen tortuosity factor defined in this manner is 1.8 times larger than in the bulk regime for a solid with 0.10 void fraction. Even at high void fractions ($\sim$0.42), the two extreme values of tortuosity factor differ by a factor of $\sim$1.4. These apparent effects of diffusion mechanism on tortuosities reflect the inaccurate use of number-averaged chord lengths when tracer reflections from random obstacles obey the Knudsen cosine law for diffuse reflection. A corrected length scale, first proposed by Derjaguin, leads to tortuosity factors independent of K_n for void fractions above 0.20; tortuosities differ by only 18% and 4% between Knudsen and bulk regimes even for void fractions of 0.10 and 0.15, respectively. The residual differences at void fractions below 0.10 arise from the increasingly serial nature of the remaining voids. Thus, a long-standing inconsistency between the defined geometric nature of tortuosity factors and their inexplicable dependence on diffusion mechanism is essentially resolved. In practice, these simulations allow the consistent and accurate use of tortuosity factors determined at any value of K_n for all diffusion regimes; they also prescribe, rigorously for void fractions above 0.15 and empirically for lower void fractions, the length scale relevant to diffusion in the Knudsen and transition diffusion regimes.

Keywords: Simulation; Transport processes; Porous media; Diffusion; Tortuosity; Monte Carlo

1. Introduction

Detailed knowledge of transport properties of porous materials is required for the design and synthesis of adsorbents, membranes, catalyst pellets, and chemical reactors. The void space within typical porous solids consists of labyrinths of contorted interconnected paths with irregular cross-sections. These morphological details control the rate at which molecules traverse macroscopic regions within the void space to allow separation, adsorption, and chemical reactions to occur. The precise details of the void structure, together with the prevailing conditions of pressure and temperature and the identity of the diffusing molecules, determine transport rates. The complex geometry and connectivity of the void space typically precludes rigorous treatments of mole and energy balances within porous solids.

Transport mechanisms depend on pore size distributions, which cause local variations in diffusion rates and prevent rigorous averaging of diffusion rates within the void space. Diffusion occurs via bulk or Knudsen processes, controlled

* Corresponding author. Tel.: +1-510-642-9673; fax: +1-510-642-4778.
E-mail address: iglesia@cchem.berkeley.edu (E. Iglesia).

0009-2509/$ - see front matter © 2004 Published by Elsevier Ltd.
doi:10.1016/j.ces.2004.04.028

by molecule–molecule or molecule–wall collisions, respectively, depending on the distance between collisions, set by the mean free path or the relevant pore dimensions. In many cases, redirecting collisions occur both among molecules and with pore walls, leading to transition regime diffusion, generally described by the treatment of Bosanquet (1944). Clearly, the nature of the pore space influences transport by dictating both the nature of the redirecting collisions and the availability and directness of paths (chords) across macroscopic regions within the void space.

A tortuosity factor (Satterfield, 1970; Wakao and Smith, 1962) is typically used to describe the longer connecting path imposed by obstacles within porous solids relative to that for motion in unconstrained free space. It is meant to reflect solely the geometry of the void space. This geometric factor, τ, is defined as

$$\tau = \frac{\phi \bar{D}}{D_e}. \tag{1}$$

Here, ϕ is the void fraction, D_e is the effective diffusivity in the porous solid, and $\bar{D}$ is a reference or equivalent diffusivity, typically described by the Bosanquet equation

$$\bar{D} = \left(\frac{1}{D_b} + \frac{1}{D_K} \right)^{-1}. \tag{2}$$

This reciprocal additivity relation describes how diffusivity depends on the bulk, D_b, and Knudsen, D_K, components when both wall and molecule collisions redirect paths. The value of D_b is given by kinetic theory (Kennard, 1938)

$$D_b = \frac{\lambda v}{3}, \tag{3}$$

where λ is the mean free path and v the mean molecular velocity. The value of D_K for an equivalent capillary is given by the treatment of Knudsen (1909)

$$D_K = \frac{\langle l_p \rangle v}{3}, \tag{4}$$

where $\langle l_p \rangle$ is the number-averaged pore diameter. The prevalent diffusion mechanism depends on the Knudsen number, K_n,

$$K_n = \frac{\lambda}{\langle l_p \rangle} \tag{5}$$

which reflects the ratio of molecule–wall to molecule–molecule collisions; thus, redirecting collisions among molecules predominate for $K_n \ll 1$ (bulk diffusion) and between molecules and pore walls for $K_n \gg 1$ (Knudsen diffusion). Substitution of Eqs. (3)–(5) into Eq. (2) yields

$$\bar{D} = \frac{D_b}{1 + K_n} \tag{6}$$

which becomes Eqs. (3) and (4) for small and large values of K_n, respectively.

Connectivity, shape, and specific limiting constrictions influence the nature of the interconnecting paths, and thus tortuosity factors, which when defined and measured properly, depend solely on the void space geometry, and not on the nature of the redirecting collisions that contribute to diffusive transport. Structural models of varying fidelity and complexity are used to describe porous solids; some constructs rely on dusty-gas concepts (Mason and Malinauskas, 1983) or capillary networks (Bhatia, 1986; Burganos and Sotirchos, 1987; Dullien, 1975; Hollewand and Gladden, 1992; Reyes and Jensen, 1985; Vocka and Dubois, 2000), which allow analytical treatments. Neither suspended "dust" particles nor intersecting or parallel cylinders, even those with irregular cross-section, provide faithful descriptions of typical void structures. These models neglect geometric details, such as constrictions, finite volumes at pore intersections, random distortions of cylindrical cross-sections, and the specific connectivity among various components in a pore size distribution. The significant impact of pore size and connectivity on measured tortuosities was previously described (Carniglia, 1986; Latour et al., 1995; Lorenzano-Porras et al., 1994; Portsmouth and Gladden, 1992; Salmas and Androutsopoulos, 2001; Vervoort and Cattle, 2002). Pore size distributions, however, provide incomplete descriptions of the connectivity among voids, which are essential to describe transport dynamics in porous solids.

We note, with some concern, that tortuosity factors are often much larger for Knudsen diffusion than for bulk diffusion, in spite of their intended and purely geometric nature. Computational studies of (non-reactive) diffusive processes in pixelized porous media (Burganos, 1998), stackings of tissues (Vignoles, 1995), anisotropic particulate arrangements (Tassopoulos and Rosner, 1992), as well as measurements in NaX zeolite beds (Geier et al., 2002) have inexplicably concluded that tortuosity factors depend on the mechanism of diffusion. Two-dimensional lattice simulations have suggested that tortuosity factors during reaction actually depend on reaction rates (Sharratt and Mann, 1987), but Zhang and Seaton (1994) later showed that effective diffusivities are the same with or without chemical reaction, except for very fast reactions or those occurring in bimodal structures. The concept of a purely geometric tortuosity factor cannot be reconciled with many of these findings.

Here, we show that geometric tortuosity factors, when properly defined and calculated, become independent of diffusion mechanism, at least for void fractions well above the percolation threshold, in random aggregates that provide faithful structural models of random porous solids. As multiple randomly connected paths become unavailable near the percolation threshold, we become unable to accurately define an equivalent Knudsen diffusivity without specific details about how various components in the pore size distribution are connected to each other; these details are seldom available. Persistent differences between tortuosity factors estimated from Knudsen and bulk diffusion occur only at void fractions much lower than those in typical catalysts and adsorbents; in such solids, even the continuum assumption required for the definition of diffusivity is likely to fail.

Here, we first describe the computational methods used to generate realistic porous structures and to monitor diffusive

processes within them. Then, we verify the validity of the Bosanquet treatment for transition diffusion in straight long cylinders and use Monte Carlo methods to estimate effective diffusivities for a wide range of K_n in realistic model pore structures. The conventional method for estimating tortuosities is modified by using a characteristic length scale for Knudsen diffusivities first proposed by Derjaguin (1946); it accounts for path length distributions and for redirections after collisions with pore walls. This approach leads to tortuosities that become essentially independent of Knudsen number for all void fractions of practical interest. Tortuosity factors in the Knudsen and bulk diffusion regimes differ by only 18% for a void fraction of 0.10, and 4% for a void fraction of 0.15. For lower void fractions, tortuosities increase with increasing K_n, even after using the Derjaguin correction. The residual effects of pore constrictions and serial connectivity can be illustrated by considering individual tracer trajectories that reveal hindered movements in porous solids at very low void fractions. In the process, we confirm that the Bosanquet treatment of transition diffusion remains accurate for random pore structures, while we resolve the inconsistent dependence of tortuosity on Knudsen number for random solids with void fractions above 0.10 by correcting Knudsen diffusivities in random pore structures by the statistics of length scale distributions and by the nature of molecule–wall collisions.

2. Methods

2.1. Generation of model porous solids

Model porous solids are constructed using partially overlapped sphere packings and Monte Carlo methods previously described (Reyes and Iglesia, 1991a,b). The void structures resemble those in porous solids formed by sol–gel, precipitation, pyrolysis, or combustion synthesis methods. Random–loose aggregates of spheres are assembled by slow settling of spheres, dropped from random locations into a cylinder and placed at the first stable three-point contact. Central regions in this packing are isotropic and uninfluenced by wall effects; their void fraction is 0.42, in agreement with experiments (Haughey and Beveridge, 1969). Void fractions are controlled by randomly increasing sphere radii according to a distribution function (uniform or Gaussian) to simulate actual densification processes. Fig. 1 shows representative examples of randomly packed and densified aggregates of spheres. The prescribed growth of spheres leads to lower void fractions and to smaller pores.

2.2. Simulations of diffusion rates

Two methods are used in order to simulate diffusion rates in these solids. Tracer methods are based on mean-square displacements of tracer molecules and they reflect transient diffusion experiments. Flux-based test particle methods probe steady-state diffusivities.

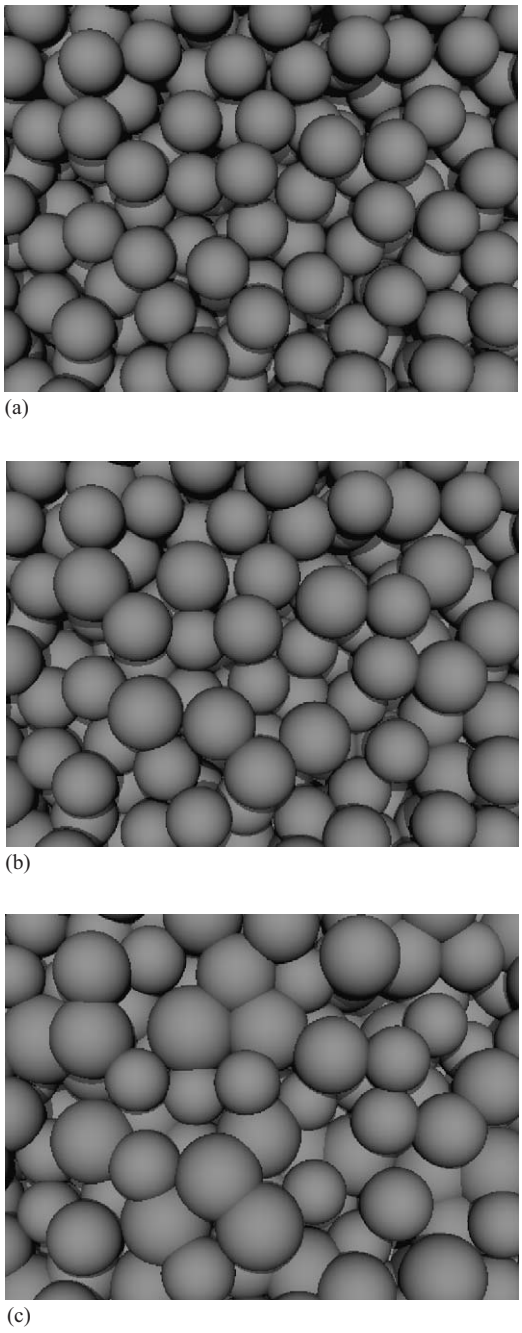

Fig. 1. Model packing structures for void fractions of 0.42 (a), 0.25 (b), and 0.10 (c).

2.2.1. Mean-square displacement methods

Tracers are initially placed at random positions within a cubic packing section with an edge length of 30 sphere diameters. Tracers falling within spheres are assigned zero displacement; this accounts for the volume excluded by the packed spheres in the effective diffusivity equation. Tracers falling within voids are moved so as to place them in random

positions at the smaller of two distances: a random distance chosen from an exponential distribution (Hildebrand, 1963) with mean λ or the distance to the nearest wall in a chosen random direction. The first type of movement leads to a random redirection, while the second leads to a reflection prescribed by the Knudsen cosine law (Greenwood, 2002; Knudsen, 1909). Elastic collisions occur at the edges of the control volume and tracer coordinates are recorded in the infinite domain as well as the actual packing section. Effective diffusivities are based on the motions of thousands of tracers with an average displacement of tens of sphere diameters in packing sections consisting of $\sim 10^5$ spheres. These conditions ensure that diffusivity estimates are not biased by incomplete sampling of the void space.

Effective diffusivities are calculated from mean square displacements using the Einstein equation (Einstein, 1926)

$$D_e = \frac{\langle R^2 \rangle}{2nt} \tag{7}$$

in which $\langle R^2 \rangle$ is the mean-square tracer displacement, n is the dimensionality of the pore space (1 for infinite cylinders and 3 for packings), and t is the time elapsed; the latter is proportional to the total cumulative distance traveled by each tracer. In all cases, distances traveled by tracers are sufficiently large so that estimated diffusivities do not depend on time.

2.2.2. Test-particle method

Effective diffusivities estimated from tracer methods can differ from steady-state diffusivities measured by flux methods for randomly connected cubic lattices (Bryntesson, 2002). Experiments have shown that steady-state diffusivities in porous slabs or industrial catalysts tend to be similar to, or slightly lower than, transient diffusivities (Baiker et al., 1982; Sotirchos, 1992). Comparisons between these two types of measurements are useful to probe any effects of pendant dead-end regions, which tracer methods tend to sample selectively when these pendant voids are placed non-randomly along conducting backbones. Test particle methods that measure steady-state diffusivities (Abbasi et al., 1983) involve the injection of a large number of tracers through an imaginary plane and determining the fraction, f_T, of these tracers that crosses another plane at a distance L (transmission) before re-crossing the injection plane

$$D_e = \frac{1}{4} f_T v L. \tag{8}$$

Tracers start from the first plane with a direction prescribed by the Knudsen cosine law and a large cube with an edge length of 30 sphere diameters is used as the control volume. At the cube sides, molecules are elastically reflected into the cube; each simulation uses at least 2×10^7 tracers. We monitor the maximum distance covered by each tracer, irrespective of whether it reaches the second imaginary place. Because a tracer with a maximum penetration depth of δ can be counted as a transmitted tracer for any $L < \delta$, this information can be used to estimate the diffusivity arising from any plane spacing less than that actually used in the simulations (Abbasi et al., 1983).

3. Results and discussion

We consider diffusion in geometrically simple systems before addressing corrections required to restore the intended geometric character of tortuosity factors for more complex porous media. First, we explore the appropriateness of Bosanquet treatments of transition diffusion; these treatments are then used to estimate equivalent diffusivities required to obtain tortuosity factors for complex porous media. Tortuosity factors for our model porous solids are estimated as a function of K_n for void fractions ranging from touching non-overlapping spheres (0.42 void fraction) to overlapped spheres near the percolation void fraction ($\sim$0.04) using Eqs. (1)–(4). The use of a reference Knudsen diffusivity first proposed by Derjaguin (1946), leads to tortuosity factors that are essentially independent of K_n for void fractions above 0.10. This reference Knudsen diffusivity is equivalent to the conventional Knudsen diffusivity, but with a characteristic length smaller than the number-averaged pore diameter or distance between collisions.

3.1. Diffusion in long cylinders

Tracer diffusion in the Knudsen regime within straight long cylinders has been examined (Beijerinck et al., 1976; Gorenflo et al., 1967) predominantly in the context of molecular flows through tubes at low pressures (Steckelmacher, 1966). The reciprocal additivity relation of Bosanquet (Eq. (2)), reminiscent of parallel resistances, is typically used for all K_n values and its theoretical basis has been demonstrated (Pollard and Present, 1948). Here, we confirm the accuracy of Eq. (2) in long cylinders, and then use it to evaluate the reference diffusivity required to estimate tortuosity factors in realistic porous constructs.

Mean-square displacements (Section 2.2.1) were used to estimate tracer diffusivities in a long cylinder for K_n values of 10^{-3}–10^3, which cover redirection mechanisms ranging from bulk to Knudsen diffusion regimes. Fig. 2a shows normalized diffusivities, $D/(R_{\mathrm{cyl}} v)$, as a function of K_n. Diffusivities given by the Bosanquet equation (solid curve) are indistinguishable from those estimated from tracer simulations (symbols). Diffusivities are proportional to K_n for low K_n values, for which redirections involve only molecule–molecule collisions. They reach a constant value for K_n values above $\sim$100. We note that these simulations reproduce exactly the predictions of the Knudsen equation, derived from kinetic theory using the same molecule–wall cosine reflection law as in our simulations (Greenwood, 2002; Knudsen, 1909).

The maximum fractional deviation from Bosanquet predictions is 0.055 for the entire K_n range (Fig. 2b). Thus, any effects of Knudsen number on tortuosity factors do not

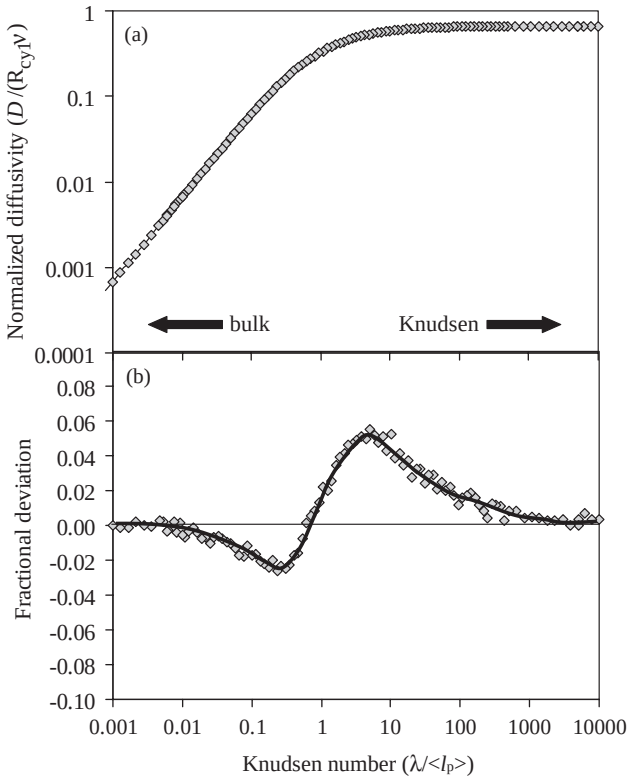

Fig. 2. Monte Carlo data for normalized diffusivities in an infinite cylinder as a function of Knudsen number and comparison with the Bosanquet formula (a) and the fractional difference between the Bosanquet formula and tracer simulations as a function of Knudsen number (b).

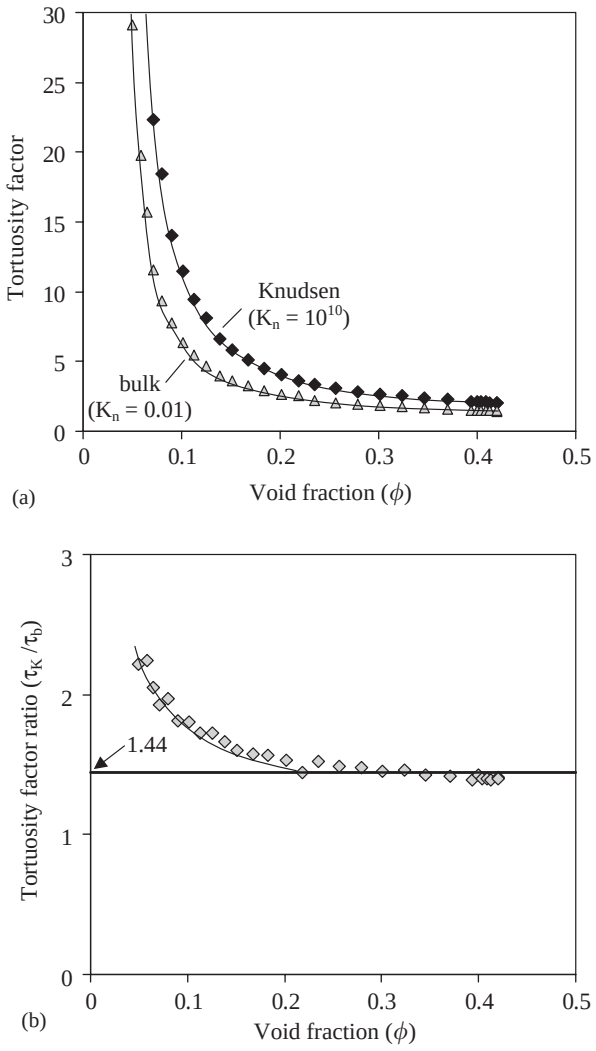

Fig. 3. Knudsen (τ_K) and bulk (τ_b) tortuosity factors as a function of void fraction for densified solids (a) and the ratio of τ_K to τ_b as a function of void fraction (b).

reflect inaccuracies in the functional dependence introduced by the Bosanquet equation in estimates of equivalent diffusivities in the transition diffusion regime. These deviations must arise instead from an inaccurate choice of characteristic length scales in the Knudsen term of Eq. (2); this length scale is conventionally, but non-rigorously, chosen as the number-averaged pore diameter and estimated from independent experiments or from the distance between collisions in tracer simulations. Next, we probe the apparent effects of K_n on tortuosity factors using this specific choice of length scale.

3.2. Tortuosity factor estimates using number-averaged pore sizes as the Knudsen diffusion length

The geometric nature of the tortuosity factor indicates that it should not depend on the diffusion mechanism, but only on the void space topology. Yet, simulations in pixelized structures (Burganos, 1998) and fiber structures (Tomadakis and Sotirchos, 1993) give tortuosities that increase with Knudsen number; these effects become stronger as void fraction decreases. Similar trends are apparent in tracer simulations within the random spherical aggregates of this study (Fig. 3). Tortuosity factors based on bulk ($K_n \ll 1$) and Knudsen ($K_n \gg 1$) diffusion are shown in Fig. 3 as a function of void fraction. The tortuosities in these two mechanistic extremes are denoted as τ_b and τ_K. These tortuosity factors are obtained by using the mean free path and the number-averaged distance between wall collisions in estimating equivalent diffusivities in the bulk and Knudsen regime, respectively.

Tortuosity factors increase monotonically with decreasing void fraction as touching spheres coalesce to form increasingly disconnected networks, which approach the percolation threshold at void fractions of ~0.04. At all void fractions, τ_b is significantly smaller than τ_K (e.g. 6.4 vs. 11.5 for 0.10 void fraction, 2.6 vs. 4.0 for 0.20, and 1.5 vs. 2.1 for 0.42), but their differences decrease as porous solids become increasingly connected with increasing void fraction. The τ_b value of 1.5 for touching spheres ($\phi = 0.42$) agrees with 1.47–1.49 values measured in randomly packed monosize spheres (Currie, 1960). Fig. 3b shows (τ_K/τ_b) ratios as

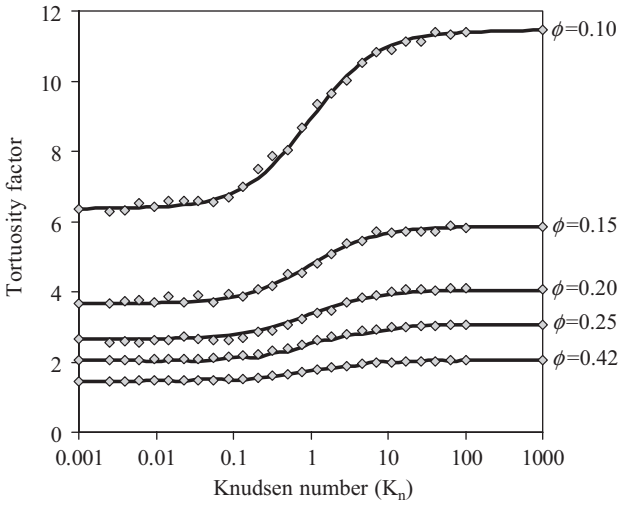

Fig. 4. Tortuosities as a function of Knudsen number for densified solids with void fractions of 0.10, 0.15, 0.20, 0.25, and 0.42.

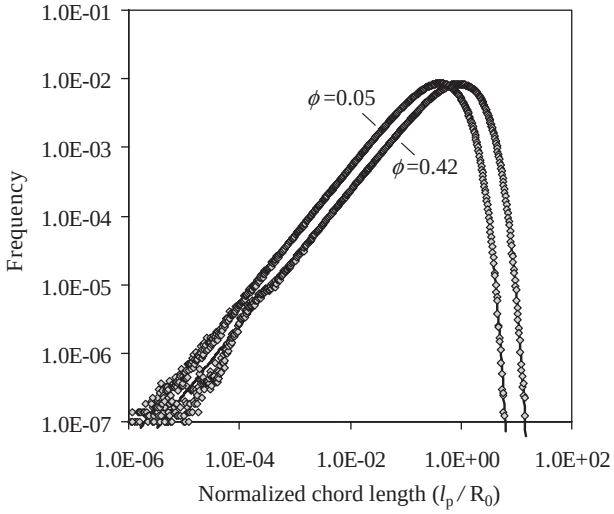

Fig. 5. Length-scale distributions for densified solids with void fractions of 0.05 and 0.42.

a function of void fraction, which approach a value of ~1.44 for void fractions above 0.15, and becomes larger as voids become poorly connected at lower void fractions.

The detailed dependence of tortuosity factors on K_n, suggested by the data in Fig. 3, is shown in Fig. 4 for five structures with void fractions between 0.10 and 0.42. These simulations indicate that a characteristic length different from the number-averaged distance between wall collisions is required in the Bosanquet equation. Once this length scale is chosen, so as to make the Knudsen and bulk tortuosities equal, the harmonic mean concepts implicit in the Bosanquet equation lead to tortuosity values independent of Knudsen number. Next, we discuss the origins of the required corrections and introduce rigorous methods for estimating the characteristic length scale relevant in the Knudsen term present within the Bosanquet equation.

3.3. Characteristic length scales in the Knudsen regime and corrections for redirection law and free path distributions

Here, the nature of the length distribution between wall collisions in the Knudsen regime and the role of redirections during wall collisions are examined using an approach first proposed by Derjaguin (1946) and later utilized by Levitz (1993, 1998). This approach shows that, in effect, the ubiquitous use of the number-averaged distance between collisions as the relevant length scale in the Knudsen and Bosanquet equations is non-rigorous for random void structures and cosine reflection laws.

Lu and Torquato (1993) showed that point tracers undergoing Knudsen diffusion within voids between impenetrable spheres follow free path distributions equivalent to the chord length distribution of the pore space (the lengths of continuous line segments in the voids when many lines are drawn at random throughout a porous solid). Further, this distribution is exponential (i.e. $P(l) = (1/\langle l \rangle)\exp(-l/\langle l \rangle)$). In our model porous solids, the distances between successive wall collisions, l_p, during Knudsen diffusion are accurately described by an exponential distribution at all void fractions, as shown in Fig. 5. Free path distributions from simulations (5×10^7 wall collisions; normalized by the radius of the initial non-overlapped spheres) for two extremes in void fraction (0.05 and 0.42; symbols) are compared with exponential distributions (lines) each with the same mean as the corresponding simulation results. These exponential distributions are identical to those predicted from kinetic theory for diffusion free paths in unconstrained space.

Although length-scale distributions for Knudsen diffusion within porous solids are similar in functional form to free path distributions for bulk diffusion, the nature of the redirection collisions differs markedly. The use of D_b as the equivalent diffusivity for small K_n is rigorous, because both free path distributions and the nature of the molecular redirections are identical to those in unconstrained space; the resulting tortuosity factor rigorously and accurately isolates the impact of pore space geometry on diffusion. In contrast, the use of D_K for a cylinder of diameter equal to the number-averaged chord length within the solid as the equivalent diffusivity for large K_n is equivalent to using the bulk diffusivity with $\lambda = \langle l_p \rangle$ (compare Eq. (4) with Eq. (3)). Collisions with surfaces, however, lead to redirections constrained to the half-space, because of the presence of solid surfaces, and redirections obey a Knudsen cosine law instead of a purely random reflection law. These considerations suggest that the use of number-averaged chord lengths for $\langle l_p \rangle$ in equivalent diffusivities is inappropriate and that tortuosity factors require an equivalent diffusivity equal to that *in free space with the same length scale distribution and type of redirections as in the porous solid.*

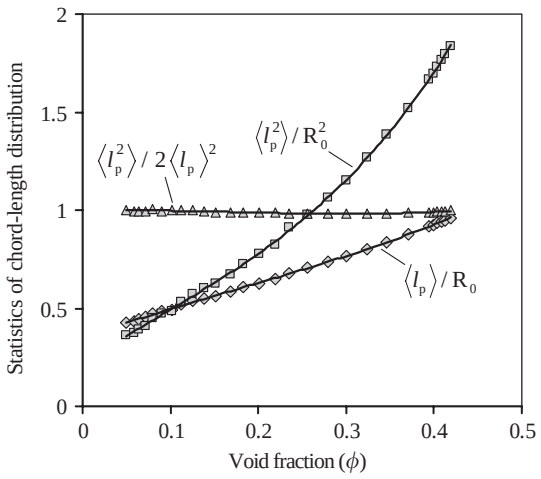

Fig. 6. Simulation results for various parameters in the Derjaguin correction, $\langle l_p\rangle$ and $\langle l_p^2\rangle$, and the ratio $\langle l_p^2\rangle/2\langle l_p\rangle$ as a function of void fraction for densified solids.

The approach of Derjaguin (1946), later extended by Levitz (1993, 1998), has led to an expression for diffusivity, D', that captures the statistics of the length-scale distribution as well as the nature of the redirecting collisions

$$D' = \frac{1}{3}\langle l_p\rangle\langle v\rangle\left[\frac{\langle l_p^2\rangle}{2\langle l_p\rangle^2} - \beta\right]. \tag{9}$$

This equation attempts to describe diffusivities through porous solids without a well-defined void structure (i.e. very spongy or porous). It describes tracer displacements as a sequence of rectilinear segments and is valid for diffusion processes in which the length and orientation of each step are uncorrelated. The Knudsen diffusion equation appears outside the brackets; it is corrected for non-exponential path distributions by the first term in brackets and for the nature of the wall reflections by the second term. The terms $\langle l_p\rangle$ and $\langle l_p^2\rangle$ are the number-averaged path length and mean-square path length, respectively. The ratio $\langle l_p^2\rangle/2\langle l_p\rangle^2$, as it appears in Eq. (9), becomes unity for exponential distributions. Simulation data for $\langle l_p\rangle/R_0$ and $\langle l_p^2\rangle/R_0^2$, where R_0 is the radius of the initial monosize spheres, are shown as a function of void fraction in Fig. 6; both quantities decrease with decreasing void fraction. The relevant ratio, $\langle l_p^2\rangle/2\langle l_p\rangle^2$, however, only varies between 0.982 and 1.003 for void fractions between 0.05 and 0.42. Consequently, this term does not give rise to significant correction for reference Knudsen diffusivities at any void fraction, because distances between collisions remain essentially exponential, even for void fractions near the percolation threshold.

The nature of the redirecting collisions is captured by the β term

$$\beta = -\sum_{m=1}^{m=\infty}\langle\cos\gamma_m\rangle \tag{10}$$

in which $\langle\cos\gamma_m\rangle$ is the average cosine of the angles between trajectory segments separated by m wall collisions. For uniform streams of molecules striking randomly placed spheres, Derjaguin showed that the Knudsen cosine law leads to

$$\langle\cos\gamma_m\rangle = (-\tfrac{4}{9})^m \tag{11}$$

and to a β value of 0.3077. For bulk diffusion, β is zero; thus, the term in square brackets in Eq. (9) becomes unity, and Eq. (9) collapses to the bulk diffusion equation (Eq. (3)). The touching and overlapping of spheres in our porous solids may lead to variations in β. For Knudsen diffusion in an infinite cylinder, we find that $\langle l_p^2\rangle/2\langle l_p\rangle^2$ is 0.666, indicating that the chord-length distribution is not exponential, and β is 0.333; their difference represents a correction factor of 0.333 that correctly reproduces Eq. (4) because diffusion occurs only in the axial direction for a cylinder, while it occurs in all three dimensions in a porous solid. We have calculated β values for porous structures with void fractions between 0.05 and 0.42 using the first 12 terms in Eq. (10) and 3×10^7 wall collisions, from which $\langle\cos\gamma_m\rangle$ terms were determined from the appropriate angles between trajectory segments. Table 1 shows simulation results for $\langle\cos\gamma_1\rangle$ up to $\langle\cos\gamma_{12}\rangle$, together with predictions from Eq. (11). Tracer simulations show the expected alternating sign and dampened decay of the $\langle\cos\gamma_m\rangle$ term; fluctuations decay more weakly with subsequent collisions than predicted by Eq. (11). This indicates that touching and overlapping spheres retain correlations among collisions longer than spheres randomly levitated in space, apparently as a result of the touching requirements used to place them within the packing. The last row of Table 1 shows the values of β computed using Eq. (10) for values of m up to 12. The fractional deviation between β values for 0.42 void fraction and the Derjaguin limiting value of 0.3077 is 0.018. The value of β increases with decreasing void fraction from 0.302 for a void fraction of 0.42 to 0.348 for a void fraction of 0.10. These values of β differ by less than 5% from those estimated using the first 50 terms of Eq. (10).

We have also tested the uncorrelated nature of path lengths by storing the time sequence of path lengths, l_p, for each tracer in diffusion simulations for K_n of 10^{10} and considering a total of 3×10^7 segments. At each void fraction, the path lengths recorded in the solid were used in diffusion simulations within unconstrained free space, from either the same sequence for each tracer as they sequentially occur in the solid ($D_{\text{free}}^{\text{ordered}}$) or by choosing randomly from the path length distribution ($D_{\text{free}}^{\text{randomized}}$). Table 2 shows $D_{\text{free}}^{\text{ordered}}/(R_0 v)$ and $D_{\text{free}}^{\text{randomized}}/(R_0 v)$. Fractional deviations between random and sequenced path lengths are less than 0.01 for all void fractions, suggesting that any correlations among successive paths do not influence transport rates. These findings do not preclude serial connectivity, especially relevant at low void fractions, which leads to repetitive sampling of local regions and to infrequent transitions to other voids to which a given region is poorly connected because openings are small and connected in series. The consequences of seriality as we approach the percolation

Table 1
Values of the average cosines of angles formed by trajectory segments separated by $1, 2, 3, \ldots, 12$ wall collisions as a function of void fraction and comparison with the theoretical prediction given by Eq. (11)

	Theory	$\phi = 0.07$	$\phi = 0.10$	$\phi = 0.15$	$\phi = 0.20$	$\phi = 0.30$	$\phi = 0.42$
$\langle \cos \gamma_1 \rangle$	−0.4444	−0.4443	−0.4446	−0.4444	−0.4445	−0.4445	−0.4445
$\langle \cos \gamma_2 \rangle$	0.1975	0.1975	0.1965	0.1983	0.2019	0.2099	0.2283
$\langle \cos \gamma_3 \rangle$	−0.0878	−0.1275	−0.1234	−0.1214	−0.1218	−0.1251	−0.1394
$\langle \cos \gamma_4 \rangle$	0.0390	0.0656	0.0622	0.0611	0.0619	0.0668	0.0852
$\langle \cos \gamma_5 \rangle$	−0.0173	−0.0498	−0.0456	−0.0432	−0.0426	−0.0448	−0.0600
$\langle \cos \gamma_6 \rangle$	0.0077	0.0274	0.0244	0.0230	0.0230	0.0258	0.0421
$\langle \cos \gamma_7 \rangle$	−0.0034	−0.0239	−0.0208	−0.0189	−0.0178	−0.0190	−0.0331
$\langle \cos \gamma_8 \rangle$	0.0015	0.0135	0.0115	0.0103	0.0099	0.0115	0.0254
$\langle \cos \gamma_9 \rangle$	−0.0007	−0.0134	−0.0113	−0.0096	−0.0088	−0.0093	−0.0216
$\langle \cos \gamma_{10} \rangle$	0.0003	0.0077	0.0062	0.0051	0.0050	0.0058	0.0178
$\langle \cos \gamma_{11} \rangle$	−0.0001	−0.0087	−0.0069	−0.0056	−0.0052	−0.0053	−0.0158
$\langle \cos \gamma_{12} \rangle$	0.0001	0.0048	0.0038	0.0029	0.0030	0.0035	0.0136
β[a]	0.3077	0.3511	0.3481	0.3424	0.3359	0.3248	0.3022

[a] β is approximated as—$\sum_{m=1}^{m=12} \langle \cos \gamma_m \rangle$.

Table 2
Normalized effective diffusivities for cases in which the path lengths for tracers in our model porous solids are used in bulk diffusion simulations in free space

	$\phi = 0.07$	$\phi = 0.10$	$\phi = 0.15$	$\phi = 0.20$	$\phi = 0.30$	$\phi = 0.42$
$D_{\text{free}}^{\text{ordered}}/(R_0 v)$	0.150	0.165	0.188	0.208	0.252	0.320
$D_{\text{free}}^{\text{randomized}}/(R_0 v)$	0.148	0.165	0.188	0.210	0.253	0.311
$D_{\text{free}}^{\text{ordered}}/D_{\text{free}}^{\text{randomized}}$	1.011	0.996	0.999	0.993	0.995	1.030

The same sequence of path lengths for each tracer was used as in the packing, or path lengths were drawn randomly from the set of all values.

threshold and few remaining paths traverse macroscopic regions in the void space are addressed in Section 3.6. Next, we use the length scales and equivalent diffusivity expression of Derjaguin to eliminate effects of K_n on tortuosity factors for most of the useful void fraction range in random porous structures ($\phi > 0.10$).

3.4. Equivalent diffusivities and tortuosity factors using Derjaguin's equation

Fig. 7 shows tortuosity factors obtained from bulk (triangles) and Knudsen (diamonds) diffusion tracer simulations, in which equivalent diffusivities are estimated from the Derjaguin equation (Eq. (9)) instead of the Knudsen term (Eq. (4)) in the Bosanquet equation. Tortuosity factors become essentially independent of diffusion regime for large void fractions; specifically, differences become less than 18% for void fractions above 0.10. For void fractions between 0.10 and 0.42, the void space is connected via multiple paths, which lead to uncorrelated chord lengths and angles (as required by the Derjaguin treatment) and to infrequent limiting small constrictions serially connected. Thus, the Derjaguin treatment resolves remaining concerns about the geometric nature of tortuosity factors and provides a rigorous protocol for choosing the relevant length scale in Knudsen and transition regimes, at least for the range of void fractions (0.10–0.42) relevant to practical porous adsorbents and catalysts, which require the accessibility provided by such well-connected structures.

Fig. 8 shows tortuosity factors as a function of Knudsen number for the same porous solids as in Fig. 4. These tortuosity factors are estimated from tracer simulations by using the Derjaguin form of the equivalent Knudsen diffusivity (Eq. (9)) where it appears in the Bosanquet equation (Eq. (2)). This approach leads to tortuosity factors that are insensitive to Knudsen number for all void fractions above 0.15 and which change by less than 18% throughout the entire K_n range for void fractions above 0.10. Thus, previously reported and unexplained dependencies of tortuosity factors on Knudsen numbers when conventional Knudsen components were inaccurately used in the Bosanquet equation (as shown in Fig. 4) essentially disappear for all practical void fractions. Tokunaga (1984) has shown that the Bosanquet relation holds for any free path and chord length distributions. Our simulations confirm the rigorous nature of the harmonic averaging implied by the Bosanquet treatment and provide a fundamental correction to the length scale relevant for the Knudsen component in this averaging. In the process, these findings resolve long-standing inconsistencies apparent from the strong effects of Knudsen number on tortuosity factors, even when such factors should reflect only

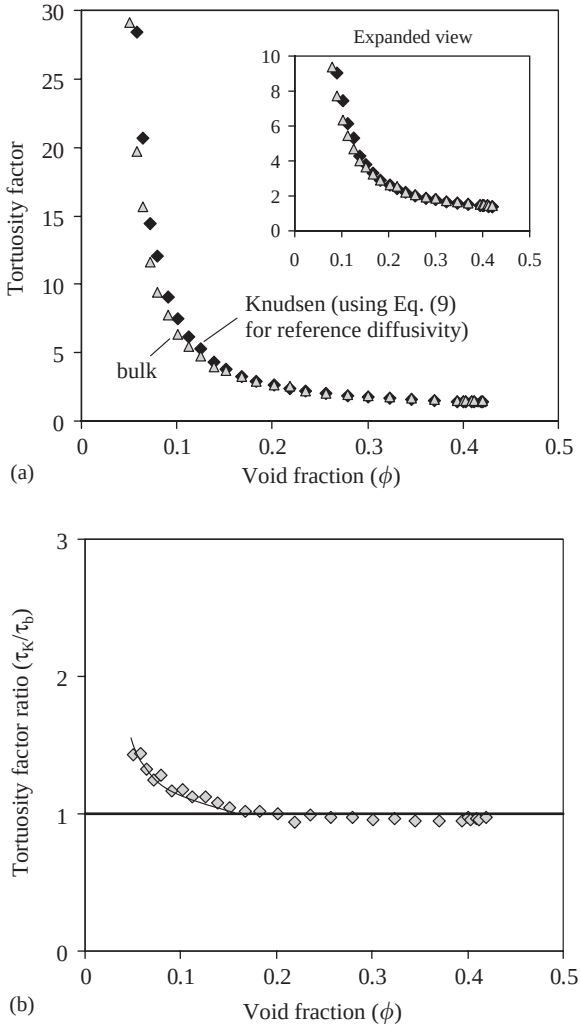

Fig. 7. Knudsen (τ_K) and bulk (τ_b) tortuosity factors as a function of void fraction, using the corrected form of the Knudsen diffusivity (Eq. (9)) in the Bosanquet formula (a) and the ratio of τ_K to τ_b as a function of void fraction (b).

the geometry of the void space.

3.5. Estimating the relevant length scale for Knudsen diffusion using experimental data

Chord-length distributions and specifically the connectivity among the various components in these distributions are not available from independent measurements for relevant porous structures. Model-dependent pore size distributions can be measured using condensation or porosimetry methods, but they require specific geometric assumptions about the void space and tend to selectively weigh the largest or the smallest pores in the structure (Henrion and Leurs, 1977; Lowell, 1979). Thus, it appears worthwhile to explore whether number-averaged chord lengths can be estimated from less equivocal measurements, and then converted to the relevant length using the Derjaguin expression (Eq. (9)).

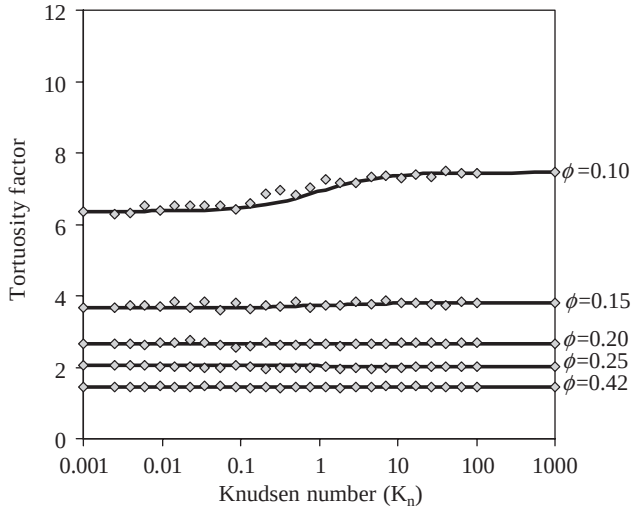

Fig. 8. The void tortuosity factor, using the corrected form of the Knudsen diffusivity (Eq. (9)) in the Bosanquet formula, as a function of Knudsen number for void fractions of 0.10, 0.15, 0.20, 0.25, and 0.42.

Mean pore sizes can be estimated from void fractions and surface areas per unit volume, S_V, based on simple geometric arguments

$$\langle l_p \rangle_{\text{estimated}} = \frac{4\phi}{S_V}. \tag{12}$$

These estimates require simple measurements of the pore volume and the exposed surface area. We have tested the accuracy of Eq. (12) for our model porous solids; in doing so, we estimate S_V by placing large numbers of tracers randomly on sphere surfaces and determining how many reside within voids. Fig. 9 shows the ratio of the number-averaged chord length, $\langle l_p \rangle_{\text{simulation}}$, from tracer measurements in the Knudsen regime ($K_n = 10^{10}$) to that given by Eq. (12). The maximum fractional deviation from unity is 0.03 throughout the entire void fraction range.

The relevant length scale for Knudsen diffusion in our packings is smaller than the number-averaged chord length. The Derjaguin equation (Eq. (9)) defines the characteristic length scale to use, with the term in square brackets giving the appropriate fraction of the number-averaged chord length (compare Eq. (9) with Eq. (4)). This ratio is shown in Fig. 9 as $\langle l_p \rangle_{\text{Derjaguin}}/\langle l_p \rangle_{\text{estimated}}$. Also shown in Fig. 9 are data for $\langle l_p \rangle_{\text{proper}}/\langle l_p \rangle_{\text{estimated}}$, where $\langle l_p \rangle_{\text{proper}}$ is the length scale that renders tortuosity values independent of Knudsen number. The values for $\langle l_p \rangle_{\text{Derjaguin}}/\langle l_p \rangle_{\text{estimated}}$ agree well with $\langle l_p \rangle_{\text{proper}}/\langle l_p \rangle_{\text{estimated}}$ for most void fractions, as expected. Near the percolation threshold, the proper ratio decreases sharply, indicating that the Derjaguin correction is insufficient for such solids. In fact, values of $\langle l_p \rangle_{\text{proper}}$ tend to zero near the percolation threshold, because transport becomes predominantly serial and tracers must traverse the smallest opening in an exponential pore size distribution, as we discuss further in Section 3.6.

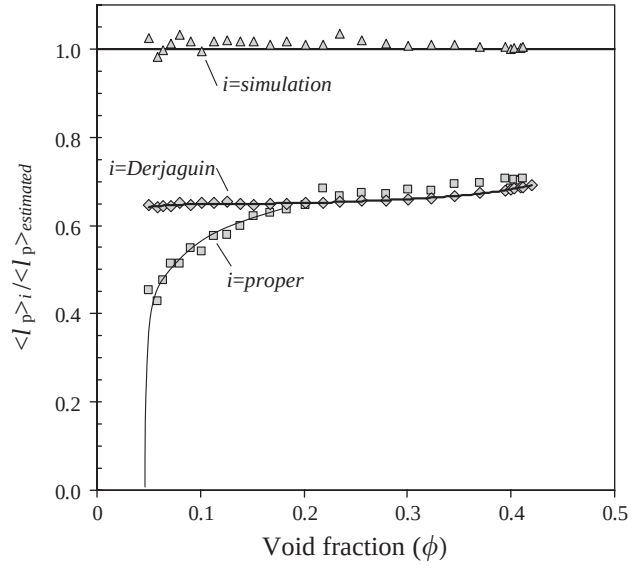

Fig. 9. Comparison of the mean pore size from simulations (i=simulation), the relevant length scale suggested by the Derjaguin equation (Eq. (9)) (i = Derjaguin), and the length scale that yields $\tau_K = \tau_b$ using the conventional tortuosity factor definition (Eqs. (1)–(4)) (i = proper), with the mean pore size estimated from Eq. (12).

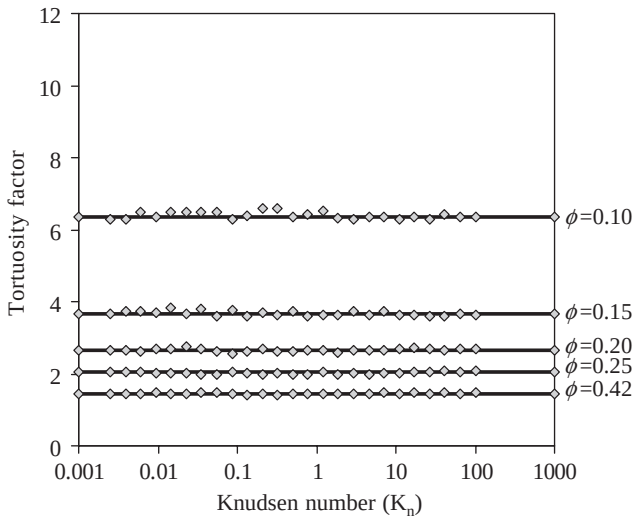

Fig. 10. The void tortuosity factor, using the conventional definition given by Eqs. (1)–(4) but with a characteristic pore size chosen so that $\tau_K = \tau_b$, as a function of Knudsen number for void fractions of 0.10, 0.15, 0.20, 0.25, and 0.42.

The results shown in Fig. 9 provide practical guidance in choosing the correct length scale required for equivalent diffusivities estimated from the Bosanquet equation (Eq. (2)), which are required to rigorously define geometric tortuosities (Eq. (1)). Effective diffusivities can be estimated from Eq. (1) by using mechanism-independent and purely geometric tortuosity factors obtained from measurements at any value of the Knudsen number and rigorously applicable at all conditions of temperature, pressure, and Knudsen number. Fig. 10 shows tortuosity factors for several model porous solids as a function of Knudsen number, where the conventional definition of the tortuosity factor (Eqs. (1)–(4)) is used with the characteristic pore size taken to be $\langle l_p \rangle_{\text{proper}}$. The independence of the tortuosity factor from diffusion regime is immediately clear; the largest variation of any of the data points is 3.3%.

3.6. Parallel versus serial transport and the effect of pore constrictions

Here, we examine the underlying basis for the residual inaccuracies in the Derjaguin equation at void fractions lower than 0.10, which lead to τ values that increase with increasing K_n. For solids with high void fractions, in which the pore space is well-connected, the relevant length scale for Knudsen diffusion is essentially proportional to that estimated from Eq. (12), because transport through these structures occurs essentially via random sampling of multiple parallel paths. Previous studies have considered diffusion in voids (Horgan, 1999) and conduction through porous solids (Staggs, 2002) as combinations of serial and parallel conducting networks, but without rigorous guidance as to their relative contributions in realistic solids. The decreasing density of connecting paths as void fraction decreases forces tracers to sample the chord length distribution in increasingly serial fashion. In fact, near the percolation threshold the continuum approximation required for the validity of effective medium diffusivities becomes invalid (Zhang and Seaton, 1992). At the percolation threshold, the one remaining connecting path becomes unavailable this remaining path is highly constricted and tortuous and it contains, in a serial arrangement, every chord length in the distribution. In this case, chord length averaging for diffusive purposes requires a relevant length scale given by $\langle l_p^{-1} \rangle^{-1}$, properly corrected for the reflection law, instead of $\langle l_p \rangle$. The value of $\langle l_p^{-1} \rangle^{-1}$ is zero, however, for any exponential distribution and thus the tortuosity factor approaches infinity at the percolation threshold.

One possible reason for the persistent effects of K_n on τ after the Derjaguin correction is the effect of an increasing density of pendant dead-end voids, which become prevalent as void fraction decreases. These pendant regions may be sampled differently in tracer measurements than in flux-based steady-state diffusion measurements. Intuitively, this arises because tracers probe dead-ends, wasting steps and time otherwise used for net motion, while molecules at steady-state are replaced on average by another molecule as they enter such pendant regions. If pendant regions artificially delay tracers and if such regions favor the larger chord lengths in the distribution, tracer simulations could lead to artificially high tortuosity factors as void fraction decreases and thus account for the residual effects of K_n on τ.

Table 3 shows effective diffusivities estimated from mean-square displacement (tracer) methods and from

Table 3
Comparison of normalized effective diffusivities obtained from the test-particle method and the mean-square displacement method at several void fractions

	$\phi = 0.06$	$\phi = 0.07$	$\phi = 0.10$	$\phi = 0.15$	$\phi = 0.20$	$\phi = 0.30$	$\phi = 0.42$
$D_{TPM}/(R_0 v)$	1.79E-04	4.78E-04	1.45E-03	4.89E-03	1.03E-02	2.83E-02	6.48E-02
$D_{MSD}/(R_0 v)$	1.91E-04	4.86E-04	1.46E-03	4.83E-03	1.04E-02	2.86E-02	6.56E-02

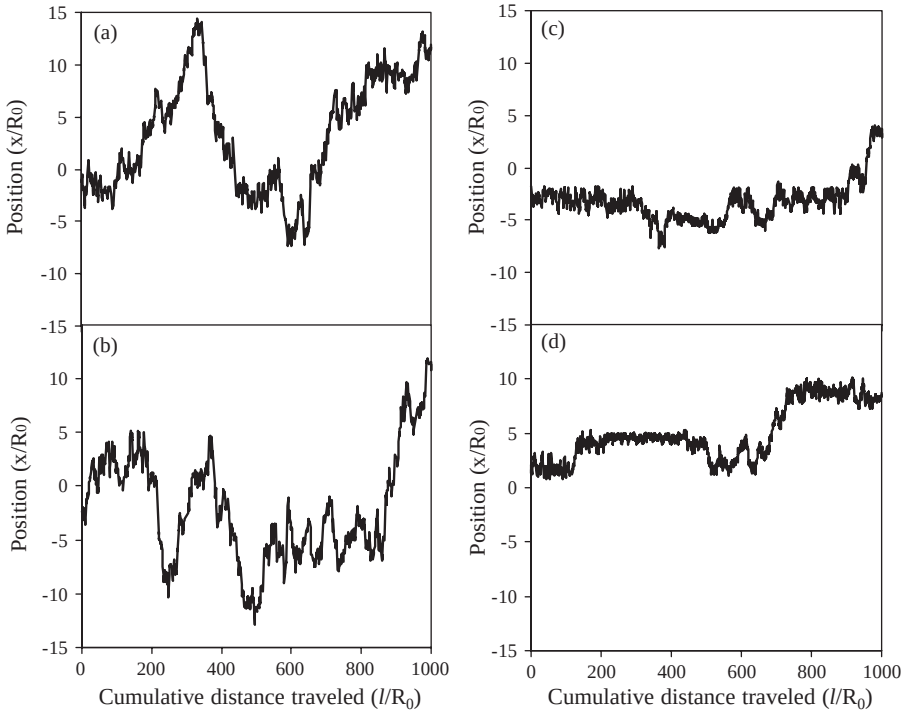

Fig. 11. Position data (x-direction) as a function of cumulative distance traveled for typical trajectories in model porous solids with $\phi = 0.42$ (a)–(b) and $\phi = 0.07$ (c)–(d).

test-particle (steady-state) methods. For all void fractions shown, the test-particle method yields virtually identical diffusivities to those obtained from tracer simulations. The maximum fractional deviation between the two methods is 0.012 at a void fraction of 0.42, 0.017 at a void fraction of 0.07 and 0.067 at a void fraction of 0.06. Note that for $\phi = 0.06$ the corrected Knudsen tortuosity factor is still ~45% greater than that based on bulk diffusion simulations, so these effects fail to offer a satisfactory explanation. There are clearly no significant differences between Knudsen diffusivities estimated from the test-particle method and the mean-square displacement method for our model porous solids. Bulk diffusion simulations using the test-particle method are not possible, even using a first-passage time approach, because of the number of tracers required for statistical significance at separation distances of 20–30 sphere diameters.

Although there are no significant correlations among successive chord lengths at any void fractions (see Table 2 and related text), pore constrictions and connectivity effects may lead to spatial correlations among successive locations where wall collisions occur. Pore constrictions have been investigated theoretically in an alternating sequence of cylinders of two different diameters (Haynes and Brown, 1971; Smith, 1986b), and in periodically constricted pores with convex or concave walls that are readily defined by arrangements of spheres (Kanellopoulos et al., 1983; Nakano et al., 1987; Smith, 1986a). The presence of pore constrictions can lead to repeated probing of a pore volume with transitions to neighboring volumes through a constriction occurring only infrequently. Such behavior can be illustrated in our model porous solids by plotting positional data for individual tracers as a function of cumulative distance traveled. Note that it is necessary to consider individual tracers for this purpose because averaging over a population of tracers will erase any differences and simply lead to Gaussian concentration profiles associated with diffusion processes. Fig. 11 shows the normalized x-coordinate as a function of cumulative distance traveled by each tracer (i.e. simulation time) for representative tracers in solids with $\phi = 0.42$

(a)–(b) and $\phi = 0.07$ (c)–(d). For $\phi = 0.42$, both sample trajectories exhibit significant variations in the locations visited, as expected for a relatively unhindered random walk in a well-connected solid. In contrast, the results for $\phi = 0.07$ show tracer movements occurring in a qualitatively uneven manner. Each tracer spends much of its time moving about a small range of positions locally, with large changes in position occurring only infrequently. This existence of 'noisy' plateaus and infrequent jumps is evident in the trajectories of many tracers, even those that ultimately experience large displacements at long times and are thus not in isolated pore volumes. We are currently considering previously developed methods (Baldwin et al., 1996; Ioannidis and Chatzis, 2000) for the geometrical characterization of our void structures and for the quantification of pore necks and connectivity within them.

4. Conclusions

Monte Carlo methods were used to create partially overlapped spherical aggregates and estimate their transport properties when diffusion occurs in the bulk, transition or Knudsen regimes. The void spaces within these model solids are representative of materials used as adsorbents, membranes, or catalyst supports. Conventionally defined tortuosity factors increased with Knudsen number when number-averaged pore sizes were used as the characteristic length scale for Knudsen diffusion, even though the Bosanquet formula is accurate in both capillaries and complex void structures; these effects of K_n reflect an improper choice of relevant length scale for Knudsen diffusion. For all of our model porous solids, the distribution of path lengths for Knudsen diffusion is well described by an exponential distribution. We showed that using a more rigorous Knudsen length scale first derived by Derjaguin led to tortuosity factors that vary by less than 4% for K_n values between 10^{-3} and 10^{10} for void fractions above 0.15, and by less than 18% for void fractions above 0.10; these void fractions cover most porous solids used in adsorption and heterogeneous catalysis. This correction to the Knudsen component accounts for the statistics of the chord-length distribution and for the nature of the tracer redirections; it is equivalent to choosing a length scale that is smaller than the number-averaged pore diameter, $\langle l_p \rangle$. At high void fractions ($\sim$0.42), the pore space is well-connected, diffusive transport occurs via a combination of parallel and series processes, and the relevant length scale is proportional to $\langle l_p \rangle$. For packings near the void percolation threshold (0.04), the pore space is poorly connected and transport is predominantly serial; in this region the relevant length scale is better described by $\langle l_p^{-1} \rangle^{-1}$, which tends to zero at the percolation threshold because the tracers must navigate the smallest opening along a single highly constricted and contorted path.

Notation

D	diffusivity
D_e	effective diffusivity in porous solid
D_b	bulk diffusivity
D_K	Knudsen diffusivity
$D_{\text{free}}^{\text{ordered}}$	free space diffusivity obtained using same sequence of path lengths for each tracer as in packing
$D_{\text{free}}^{\text{randomized}}$	free space diffusivity using path lengths drawn randomly from those in packing
D_{MSD}	effective diffusivity from mean-square displacement method (Eq. (7))
D_{TPM}	effective diffusivity from test-particle method (Eq. (8))
$\bar{D}$	equivalent diffusivity for tortuosity factor calculation
D'	Derjaguin expression for diffusivity (Eq. (9))
f_T	fraction of tracers transmitted
K_n	Knudsen number
l	cumulative distance traveled by a tracer
l_p	distance between wall collisions in Knudsen diffusion
$\langle l_p \rangle$	number-averaged pore size (i.e. mean chord length)
$\langle l_p \rangle_{\text{estimated}}$	length scale estimated from Eq. (12)
$\langle l_p \rangle_{\text{Derjaguin}}$	relevant length scale suggested by the Derjaguin expression (Eq. (9))
$\langle l_p \rangle_{\text{simulation}}$	number-averaged pore size from Monte Carlo simulation of Knudsen diffusion
$\langle l_p \rangle_{\text{proper}}$	length scale that yields $\tau_K = \tau_b$ for conventional tortuosity factor (Eqs. (1)–(4))
$\langle l_p^2 \rangle$	mean-square distance between wall collisions
L	plane spacing in test-particle method
n	dimensionality
R_0	sphere radius used for initial non-overlapping packing
$\langle R \rangle$	mean tracer displacement
$\langle R^2 \rangle$	mean-square tracer displacement
R_{cyl}	radius of infinite cylinder
S_V	surface-to-volume ratio
t	elapsed time

Greek letters

β	correction term related to statistics of tracer redirections
γ_m	angle between trajectory segments separated by m wall collisions
λ	mean free path for gas phase
v	gas mean molecular velocity
τ	tortuosity factor
τ_K	tortuosity factor based on Knudsen diffusion
τ_b	tortuosity factor based on bulk diffusion
ϕ	void fraction

References

Abbasi, M.H., Evans, J.W., Abramson, I.S., 1983. Diffusion of gases in porous solids—Monte-Carlo simulations in the Knudsen and ordinary diffusion regimes. A.I.Ch.E. Journal 29 (4), 617–624.

Baiker, A., New, M., Richarz, W., 1982. Determination of intraparticle diffusion coefficients in catalyst pellets—A comparative study of measuring methods. Chemical Engineering Science 37 (4), 643–656.

Baldwin, C.A., Sederman, A.J., Mantle, M.D., Alexander, P., Gladden, L.F., 1996. Determination and characterization of the structure of a pore space from 3D volume images. Journal of Colloid and Interface Science 181 (1), 79–92.

Beijerinck, H.C.W., Stevens, M.P.J.M., Verster, N.F., 1976. Monte-Carlo calculation of molecular flow through a cylindrical channel. Physica B, C 83 (2), 209–219.

Bhatia, S.K., 1986. Stochastic theory of transport in inhomogeneous media. Chemical Engineering Science 41 (5), 1311–1324.

Bosanquet, C.H., 1944. British TA Report BR-507.

Bryntesson, L.M., 2002. Pore network modelling of the behaviour of a solute in chromatography media: transient and steady-state diffusion properties. Journal of Chromatography A 945 (1–2), 103–115.

Burganos, V.N., 1998. Gas diffusion in random binary media. Journal of Chemical Physics 109 (16), 6772–6779.

Burganos, V.N., Sotirchos, S.V., 1987. Diffusion in pore networks: effective medium theory and smooth field approximation. A.I.Ch.E. Journal 33 (10), 1678–1689.

Carniglia, S.C., 1986. Construction of the tortuosity factor from porosimetry. Journal of Catalysis 102 (2), 401–418.

Currie, J.A., 1960. Gaseous diffusion in porous media. Part 2: dry granular materials. British Journal of Applied Physics 11 (8), 318–324.

Derjaguin, B., 1946. Measurement of the specific surface of porous and disperse bodies by their resistance to the flow of rarified gases. Comptes Rendus (Doklady) de l'Académie des Sciences de l'URSS 53 (7), 623–626.

Dullien, F.A.L., 1975. New network permeability model of porous media. A.I.Ch.E. Journal 21 (2), 299–307.

Einstein, A., 1926. Investigations on the Theory of the Brownian Movement. Dover, New York.

Geier, O., Vasenkov, S., Kärger, J., 2002. Pulsed field gradient nuclear magnetic resonance study of long-range diffusion in beds of NaX zeolite: evidence for different apparent tortuosity factors in the Knudsen and bulk regimes. Journal of Chemical Physics 117 (5), 1935–1938.

Gorenflo, R., Pacco, M.G., Scherzer, B.M.U., 1967. Monte Carlo simulation of a Knudsen gas flow with due allowance for sojourn time. Zeitschrift fur Angewandte Physik 22 (6), 500–505.

Greenwood, J., 2002. The correct and incorrect generation of a cosine distribution of scattered particles for Monte-Carlo modelling of vacuum systems. Vacuum 67 (2), 217–222.

Haughey, D.P., Beveridge, G.S., 1969. Structural properties of packed beds—a review. Canadian Journal of Chemical Engineering 47 (2), 130–140.

Haynes, H.W., Brown, L.F., 1971. Effect of pressure on predicted and observed diffusion rates in constricted pores—theoretical study. A.I.Ch.E. Journal 17 (2), 491–494.

Henrion, P.N., Leurs, A., 1977. Influence of powder bed structure on mercury penetration response in porosimetry. Powder Technology 17 (1), 145–146.

Hildebrand, J.H., 1963. An Introduction to Kinetic Theory. Reinhold, New York.

Hollewand, M.P., Gladden, L.F., 1992. Representation of porous catalysts using random pore networks. Chemical Engineering Science 47 (9–11), 2757–2762.

Horgan, G.W., 1999. An investigation of the geometric influences on pore space diffusion. Geoderma 88 (1–2), 55–71.

Ioannidis, M.A., Chatzis, I., 2000. On the geometry and topology of 3D stochastic porous media. Journal of Colloid and Interface Science 229 (2), 323–334.

Kanellopoulos, N., Munday, K.A., Nicholson, D., 1983. The flow of a non-adsorbed, collisionless gas through linked spheres—a model for zeolite diffusion. Journal of Membrane Science 13 (2), 247–258.

Kennard, E.H., 1938. Kinetic Theory of Gases. McGraw-Hill, New York.

Knudsen, M., 1909. Die gesetze der molecularströmung und der inner reibungsströmung der gase durch röhren. Annalen der Physik 28, 75–130.

Latour, L.L., Kleinberg, R.L., Mitra, P.P., Sotak, C.H., 1995. Pore-size distributions and tortuosity in heterogeneous porous media. Journal of Magnetic Resonance, Series A 112 (1), 83–91.

Levitz, P., 1993. Knudsen diffusion and excitation transfer in random porous media. Journal of Physical Chemistry 97 (15), 3813–3818.

Levitz, P., 1998. Off-lattice reconstruction of porous media: critical evaluation, geometrical confinement and molecular transport. Advances in Colloid and Interface Science 76–77, 71–106.

Lorenzano-Porras, C.F., Carr, P.W., McCormick, A.V., 1994. Relationship between pore structure and diffusion tortuosity of ZrO_2 colloidal aggregates. Journal of Colloid and Interface Science 164 (1), 1–8.

Lowell, S., 1979. Introduction to Powder Surface Area. Wiley-Interscience, New York.

Lu, B., Torquato, S., 1993. Chord-length and free-path distribution functions for many-body systems. Journal of Chemical Physics 98 (8), 6472–6482.

Mason, E.A., Malinauskas, A.P., 1983. Gas Transport in Porous Media: The Dusty-Gas Model. Elsevier, Amsterdam.

Nakano, Y., Iwamoto, S., Yoshinaga, I., Evans, J.W., 1987. The effect of pore necking on Knudsen diffusivity and collision frequency of gas molecules with pore walls. Chemical Engineering Science 42 (7), 1577–1583.

Pollard, W.G., Present, R.D., 1948. On gaseous self-diffusion in long capillary tubes. Physical Review 73 (7), 762–774.

Portsmouth, R.L., Gladden, L.F., 1992. Mercury porosimetry as a probe of pore connectivity. Chemical Engineering Research and Design 70 (1), 63–70.

Reyes, S.C., Iglesia, E., 1991a. Effective diffusivities in catalyst pellets —new model porous structures and transport simulation techniques. Journal of Catalysis 129 (2), 457–472.

Reyes, S.C., Iglesia, E., 1991b. Monte Carlo simulations of structural properties of packed beds. Chemical Engineering Science 46 (4), 1089–1099.

Reyes, S.C., Jensen, K.F., 1985. Estimation of effective transport coefficients in porous solids based on percolation concepts. Chemical Engineering Science 40 (9), 1723–1734.

Salmas, C.E., Androutsopoulos, G.P., 2001. A novel pore structure tortuosity concept based on nitrogen sorption hysteresis data. Industrial and Engineering Chemistry Research 40 (2), 721–730.

Satterfield, C.N., 1970. Mass Transfer in Heterogeneous Catalysis. MIT Press, Cambridge, MA.

Sharratt, P.N., Mann, R., 1987. Some observations on the variation of tortuosity with Thiele modulus and pore-size distribution. Chemical Engineering Science 42 (7), 1565–1576.

Smith, D.M., 1986a. Knudsen diffusion in constricted pores—Monte-Carlo simulations. A.I.Ch.E. Journal 32 (2), 329–331.

Smith, D.M., 1986b. Restricted diffusion through pores with periodic constrictions. A.I.Ch.E. Journal 32 (6), 1039–1042.

Sotirchos, S.V., 1992. Steady-state versus transient measurement of effective diffusivities in porous-media using the diffusion-cell method. Chemical Engineering Science 47 (5), 1187–1198.

Staggs, J.E.J., 2002. Estimating the thermal conductivity of chars and porous residues using thermal resistor networks. Fire Safety Journal 37 (1), 107–119.

Steckelmacher, W., 1966. A review of the molecular flow conductance for systems of tubes and components and the measurement of pumping speed. Vacuum 16 (11), 561–584.

Tassopoulos, M., Rosner, D.E., 1992. Simulation of vapor diffusion in anisotropic particulate deposits. Chemical Engineering Science 47 (2), 421–443.

Tomadakis, M.M., Sotirchos, S.V., 1993. Ordinary and transition regime diffusion in random fiber structures. A.I.Ch.E. Journal 39 (3), 397–412.

Vervoort, R.W., Cattle, S.R., 2002. Linking hydraulic conductivity and tortuosity parameters to pore space geometry and pore-size distribution. Journal of Hydrology 272 (1–4), 36–49.

Vignoles, G.L., 1995. Modelling binary, Knudsen and transition regime diffusion inside complex porous media. Journal de Physique IV 5 (C5), 159–166.

Vocka, R., Dubois, M.A., 2000. Pore network as a model of porous media: comparison between nonhierarchical and hierarchical organizations of pores. Physical Review E 62 (4), 5216–5224.

Wakao, N., Smith, J.M., 1962. Diffusion in catalyst pellets. Chemical Engineering Science 17 (11), 825–834.

Zhang, L., Seaton, N.A., 1992. Prediction of the effective diffusivity in pore networks close to a percolation threshold. A.I.Ch.E. Journal 38 (11), 1816–1824.

Zhang, L., Seaton, N.A., 1994. The application of continuum equations to diffusion and reaction in pore networks. Chemical Engineering Science 49 (1), 41–50.